

Dedicated to Acad. Prof. Dr. Margareta Giurgea with the occasion of her 90-th anniversary

EMBEDDING JACOBSEN MANGANESE(III) SALEN COMPLEX INTO NANOPOROUS MOLECULAR SIEVES: SPECTROSCOPIC CHARACTERISATION OF HOST-GUEST INTERACTIONS

L. Frunza^{*}, I. Zgura, I. Nicolaie, A. Dittmar^a, H. Kosslick^a, R. Fricke^a

National Institute of Materials Physics, 077125-Bucharest-Magurele, P.O. Box Mg 7, Romania

^aInstitute of Applied Chemistry, Berlin, Germany

We report some spectroscopic arguments showing the guest-host interactions in the case of the composites containing Jacobsen salen complex and nanoporous molecular sieves of different types: SBA-15, MCM-48, MCM-41. The complex was embedded by impregnation, but care was given for washing out the weakly anchored part. Siliceous nanoporous materials lead to a weaker interaction than Al containing forms. Thermal analysis has shown that at least in the case of the composite containing MCM-41 the embedded complex still contain chloride ions, therefore the bonding to the surface was apical. In situ experiments indicate that the thermal stability of the embedded complex is higher than in the free state. The differences among the composites coming from the structure of the molecular sieves are discussed.

(Received July 4, 2005; accepted July 21, 2005)

Keywords: Manganese salen complex, Molecular sieves, Host-guest interactions, FTIR spectroscopy, UV-vis spectroscopy

1. Introduction

Chiral epoxides are used as building blocks for the synthesis of many pharmaceuticals and fine chemicals [1,2]. The Mn(III) salen systems are known as remarkable efficient catalysts for the synthesis of chiral epoxides [3,4]. Then, intense efforts were made to prepare the heterogeneous version of these chiral metal complexes in an attempt to make possible their recovery and recycling. Chiral manganese salen complexes have been encapsulated within the supercages of faujasites Y and EMT [5,6] or they have been immobilized on a variety of organic and inorganic matrices (e.g., some early works [7-14]).

This contribution presents some results on the host-guest interactions inherent for hydrogenising the Jacobsen complex ((R,R)-N,N'-bis(3,5-di-*tert*-butylsalicylidene)-1,2-cyclohexanediamino-manganese chloride) in nanoporous molecular sieves (MS) of the type SBA-15 or MCM-48 in comparison with MCM-41 molecular sieves. The aim was to identify the nature of the guest species and to monitor the stability of the Jacobsen complex by observing the changes during the composite heating up to 600 K. Information was given by thermal analysis, by infrared spectroscopy, especially *in situ* investigations and by UV-vis spectroscopy as well. The interaction of Jacobsen complex with the matrix surface depends on the matrix type and on the temperature (leading to the complex degradation).

* Corresponding author: lfrunza@infim.ro

2. Experimental

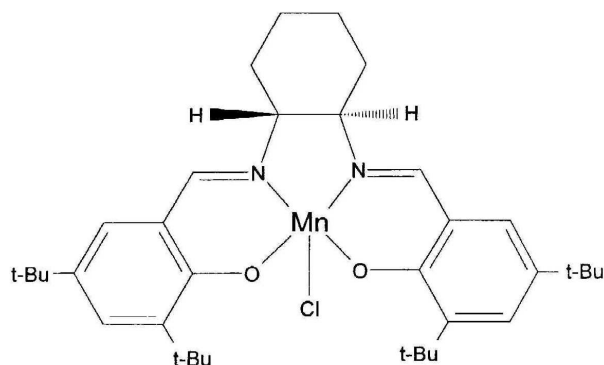


Fig. 1. Structure of Jacobsen complex. t-Bu symbolizes the *tert*-butyl group.

2.1 Materials

Jacobsen (J) complex was purchased from Aldrich and used without further purification. Its structure is sketched in Fig. 1. One can notice the chiral equatorial tetradentate salen ligand and the apical ligand (chloride ion).

Reagent grade dichloromethane (DCM) (Merck) was used as solvent.

Nanoporous molecular sieves with large pores and different structures were chosen for confinement: SBA-15 with hexagonal structure of cylindrical pores, MCM-48 with cubic 3D structure of the pores (Fig. 2), in comparison with the molecular sieve of MCM-41-type having also a hexagonal structure. These nanoporous materials were obtained in laboratory using known recipes [15-20]. They have been fully characterized by X-ray diffraction, electron microscopy, nitrogen adsorption, thermal analysis measurements. The main characteristics of these materials are given in Table 1.



Fig. 2. Pore structure of molecular sites type A) SBA-15; B) MCM-48.

Table 1. Characteristics of the composite matrices.

Molecular sieve	Oxide composition	BET surface area m^2g^{-1}	Pore volume cm^3g^{-1}	Loading degree with Jacobsen complex g per 1 g dry MS
SBA-15	Si	674	0.78	0.6
AlSBA-15	Al, Si	643	0.80	
MCM-48	Si	703	0.64	0.5
AlMCM-41(1)	Al, Si	320	0.56	3.5
AlMCM-41(2)	Al, Si	655	0.78	1.4

2.2. Embedding the complex into the nanopores

Jacobsen complex was supported by impregnation, using a solution of 15 mg complex [9] in DCM to cover 300 mg molecular sieve. After 6 h equilibration, the solvent was removed, and then the sample was carefully washed with solvent and was air-dried at 80 °C. The label of loaded sample is J/MS where MS is the actual acronym of the molecular sieve.

2.3. Methods of characterization

Thermal analysis was carried out with a Setaram TGDTA 92 apparatus from room temperature up to 800 °C under dry airflow. Mass loss and heat flow were determined.

FTIR spectra of pure or supported complexes were recorded on KBr pellets in a Nicolet Magna 550 spectrophotometer. *In situ* FTIR spectra of self-supported wafers were recorded using a quartz cell fitted with CaF₂ windows. The samples were out gassed at certain temperature under 10⁻² Pa for ½ h; after the spectrum recording, the temperature was raised with 20 °C and a new cycle of out gassing-recording-raising the temperature was applied.

UV-vis spectra of solutions were measured in quartz cuvette using a Perkin-Elmer Lambda 18 spectrometer. Diffuse reflectance spectra of powder samples were recorded on the special attachment. Kubelka-Munk function was calculated and represented in the latter case.

All the spectra were decomposed into (Gaussian) components using commercial programs.

3. Results and discussion

In order to demonstrate the encapsulation of Jacobsen compound, we used a combination of analytical techniques as follows.

3.1 TG-DTA measurements

Representative DTA plots are reproduced in Fig. 3A while the corresponding derivatives of the thermogravimetric (DTG) curves are shown in Fig. 3B. The curves in Fig. 3A indicate several endothermic and exothermic processes taking place. The latter processes are due to oxidation/decomposition of the organic guest molecules.

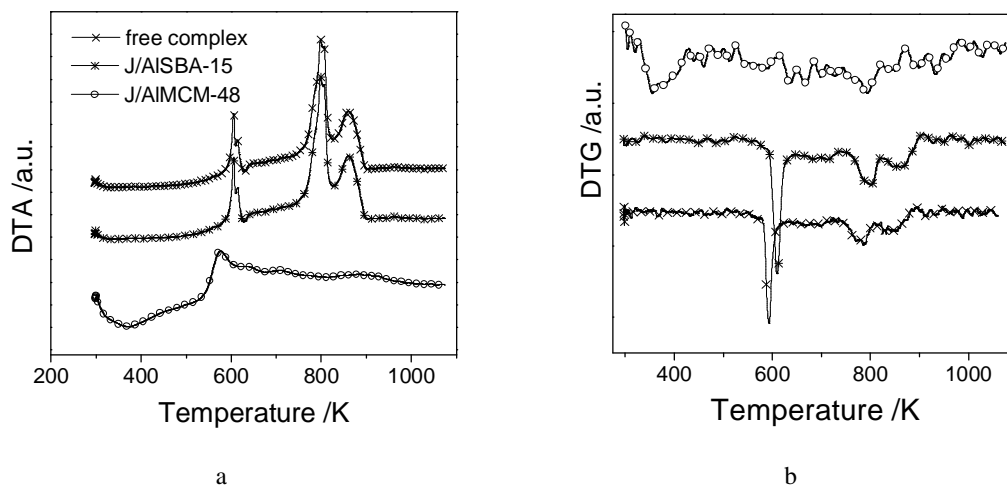


Fig. 3. DTA (A) and DTG (B) curves of the free and embedded Jacobsen complex.

DTG peaks (Fig. 3B) are asymmetric showing that there are several species contributing to the mass loss. Even though there is somehow a correspondence between DTA and DTG curves, showing that the same chemical transformations of confined Jacobsen complex take place inside the pores of the molecular sieves. However the maxima for weight loss and heat flow do not exactly correspond (especially for the embedded complex) suggesting decomposition and desorption are not simultaneous.

For the free complex, the peaks in DTG curves (corresponding to the steps in TG curves) are very well defined. It was previously supposed [9] that first hydrogen chloride (HCl) is released at 400 K; then oxidation of remaining organics takes place, such as successive cleavage and removal processes of the *tert*-butyl groups and probably of the cyclohexyl ring; finally there is the combustion of the aromatic rings. But in the absence of careful analysis of the reaction products, we can only speculate on the assignment of the DTA-DTG peaks.

Jacobsen complex loaded in molecular sieves leads to less well-defined weight loss and DTA peaks. In addition, decomposition is shifted to higher temperature up to *ca.* 50, due to a so-called stabilization of the complex inside the pores. This fact reveals strong interactions; consequently one can conclude that the complex is embedded inside the pores of the molecular sieves.

The architecture and the chemical properties of the molecular sieves are expected to strongly influence the reactivity of the complex. In addition, we expect the isomorphous substitution of Si in the framework by Al atoms more electropositive than Si influences the guest-host interaction between the Jacobsen complex and the framework. Indeed, the thermogravimetric curves in Fig. 3 show some differences among our loaded samples.

Thermogravimetric measurements allowed estimating the amount of the complex in the composites. In this aim, we considered the total mass loss from which we subtracted the mass loss due to water removal from the external surface as well as from dehydroxylation, both of these water loss being known from the study of unloaded molecular sieve. Table 1 gives the obtained values. The loading is rather low, due to the fact that the complex is easily leached. Sample J/AlMCM-41(1) is an exception from this point of view, because it was not leached.

3.2. FTIR spectroscopy

IR spectra (KBr technique) for the free and encapsulated complex in the low wavenumber range (in a region of matrix transparency) and in the range characteristic for OH groups are shown in Fig. 4 A and B, respectively.

The free Jacobsen complex and the sample highly loaded show typical absorption peaks which were attributed according to the literature [9, 21-23] as follows: at 1250-1550 cm^{-1} to CC as well as to C=N stretch vibrations of the aromatic ring or imine group. In addition, deformations of CH_2 and CH_3 groups appear at 1460 and 1380 cm^{-1} . The peak in the region 1330-1355 cm^{-1} can be assigned to $\nu(\text{C-O})$. $\text{C}_{\text{arom}}\text{H}$ stretch, CH_3 and CH_2 asymmetrical and symmetrical stretch appear at frequencies between 2800 and 3200 cm^{-1} , but they are seen only as small shoulders on the low frequency side of the very large and strong OH stretching band in Fig. 4. Characteristic bands are those of the imine stretching vibration around 1630 cm^{-1} and of metallosalen complexes at 1540 cm^{-1} [24]. The other samples show weak and undefined bands; the IR spectra in this region are irrelevant.

The main peaks in the IR spectra of J/Al-MCM-41(1) sample are shifted when comparing with free Jacobsen complex, like CH bonds in the alkyl chains and also the C=N bonds of the imine groups. These shifts are due to the interaction of the complex with the surface of the molecular sieve by encapsulation.

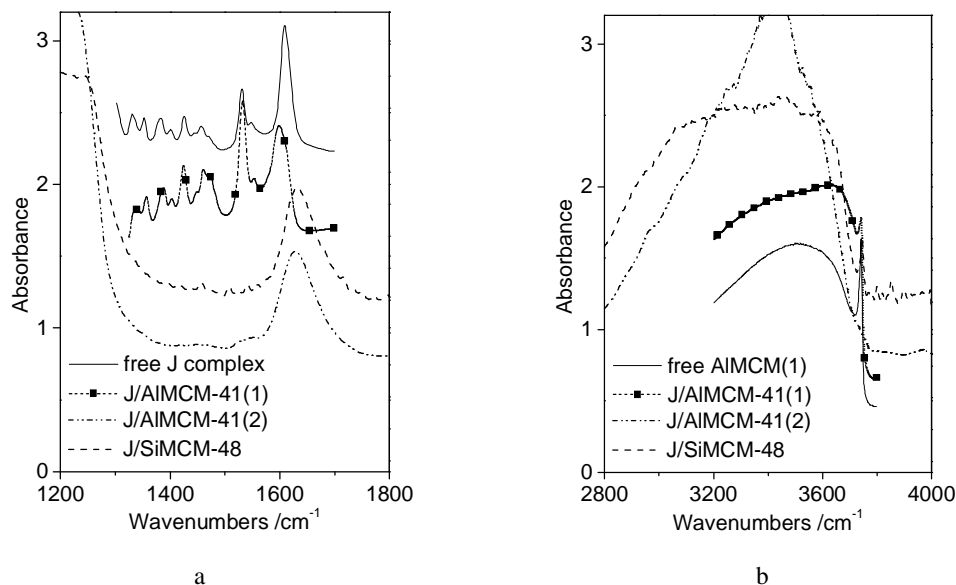


Fig. 4. IR spectra in KBr in the region of (A) deformation vibrations and (B) OH stretching vibrations.

As resulting from Fig. 4B, the height of the isolated OH groups (responsible for the absorption at 3730 cm^{-1}) is much higher on the unloaded sample than on the sample loaded with Jacobsen complex. It results that a part of these isolated OH groups participate in the interaction between the Mn complex and the surface. The downward frequency shift is higher in the case of SBA-15 than for MCM-41 materials: this seems to support the stronger interaction in the former case, due to a more favorable position of the aromatic rings against the pore walls.

In order to monitor the changes observed during the heating up and to characterize the structure of embedded complex, the composite spectra were collected *in situ*. Typical spectra are shown in Fig. 5, for the sample J/AIMCM-41(1), having the highest loading among the studied composites. The behavior of the unloaded molecular sieve is also shown for comparison. Intensity of the peak due to stretching of free OH groups (*ca.* 3730 cm^{-1}) decreases considerably by loading, indicating their interaction with (the aromatic rings of) the Jacobsen complex within the pores.

All the spectra were decomposed into Gaussian components, as shown in Fig. 6A for a region containing overtones and combination bands of the framework and imine characteristic peak. Fig. 6B and C illustrate the temperature variation of the height of some important peaks obtained by decomposition. It is noteworthy that the intensity of the framework overtones/combination bands does not change with increasing the temperature (not shown), this fact showing the goodness of the fit.

Generally, confinement restricts the atom motions leading to a slight increase of the force constants and consequently, an upward shift of the frequencies in the loaded state in comparison with those of the free state (here of the Jacobsen complex). Peaks due to deformations vibrations of CH_2 and CH_3 groups decrease in intensity with increasing temperature, faster than those due to the vibrations of the aromatic part. This obviously indicates a dealkylation process. Peaks assigned to stretching of CC_{arom} also decrease in intensity due to disappearance of these rings from the system by gradual decomposition/desorption, but the peak at 1495 cm^{-1} decreases faster than that at 1605 cm^{-1} , showing that a chemical transformation takes place. A red shift of a few cm^{-1} in the peak positions can be also observed by increasing the temperature.

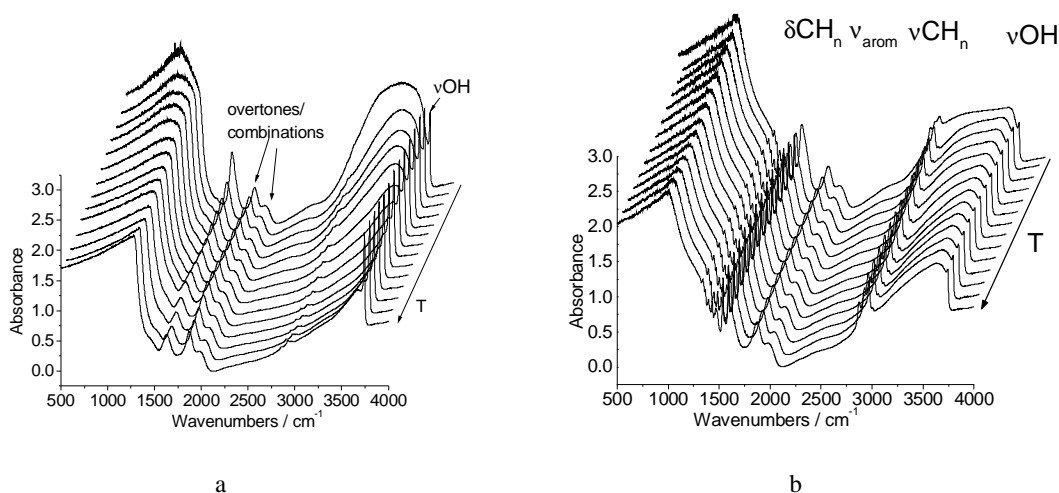


Fig. 5. *In situ* FTIR spectra of A) the empty AlMCM-41(1), B) J/AlMCM-41(1) sample at temperatures increasing from room temperature to 600 K.

The presence of some peaks at high outgassing temperatures gives also information about the thermal stability of the Jacobsen complex.

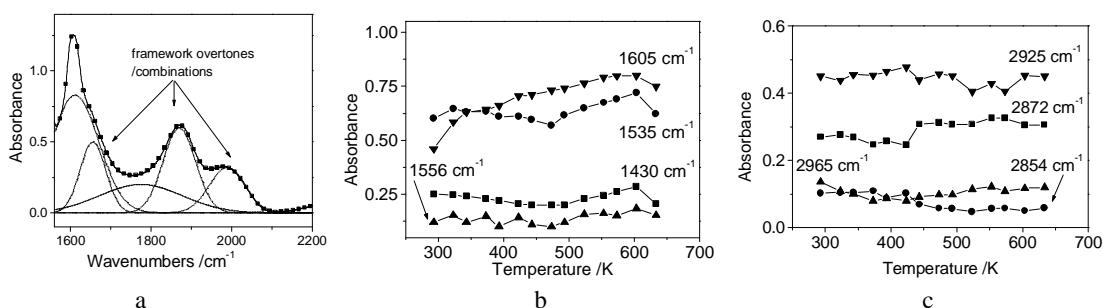


Fig. 6. Decomposition of the FTIR spectra into Gaussians (A) and the temperature variation of some characteristic peaks of J/AlMCM-41(1) (B and C).

3.3. UV-vis spectroscopy

Molecular sieves containing Jacobsen complex are light brown in color, this color arising from the strong absorption band of the Jacobsen complex at low wavelength (<350 nm) tailing to beyond 400 nm as shown in Fig. 7A for a solution in DCM. Diffuse reflectance spectra of the some of the investigated composites are presented in Fig. 7B. As results from Fig. 7, the composite spectra are more rich in bands than the free Jacobsen complex, probably due to the existence of several species with different confining environment. Each spectrum was decomposed accordingly in several Gaussians, as shown also in Fig. 7 for one of the spectra.

The color of the Jacobsen complex could also provide a spectroscopic handle for differentiating surface species. The main peaks at 490 nm (d-d) as well as ligand to metal charge transfer (CT) peak at 432 nm are shifted mostly toward the higher energy (Table 2): This shift could be consistent with the complex distortion inside the pores of the molecular sieve; in this case, these spectra are an evidence for embedding the complex inside the pores. Since Kubelka-Munk function is proportional with the concentration of the species responsible for the corresponding band, processing the spectra provides new informations on the loading level of the Jacobsen complex in

the pores and of its distortion due to guest-host interactions. Thus, one can estimate that silica surfaces retain less the complex than those containing Al ions. On the other hand, the 3D structure of MCM-48 pores does not allow a complete filling of the pores with the rather bulky molecule of the Jacobsen complex.

The tetradentate (R,R)-N,N'-bis(3,5-di-*tert*-butylsalicylidene)-1,2-cyclohexanediamino ligand of Jacobsen complex adopts a near-planar geometry around the metallic ion and therefore the complex containing the chloride ion as the five ligand approaches the structure of a square pyramid. However, such a complex easily passes at six coordination of the pseudo-octahedral type by forming adducts with electron donating atoms from surroundings (e.g. donor atoms of the solvent or of the framework). It is known that the complexes of manganese(III) ion in an octahedral environment should give rise to spin allowed absorption peaks as well as to spin forbidden ones due to its d^4 electronic structure [25]; these should exhibit a broad strong band at $16000 - 21000 \text{ cm}^{-1}$ (625-476 nm) which may be assigned, in the (pseudo)octahedral group, to the ${}^5T_{2g} \rightarrow {}^5E_g$ transition. The fairly intense crystal field band observed by us at ca. 20500 cm^{-1} (=487 nm) results probably from a combination of factors, among which there are the low symmetry of the complex ion and the low lying ligand to metal CT states.

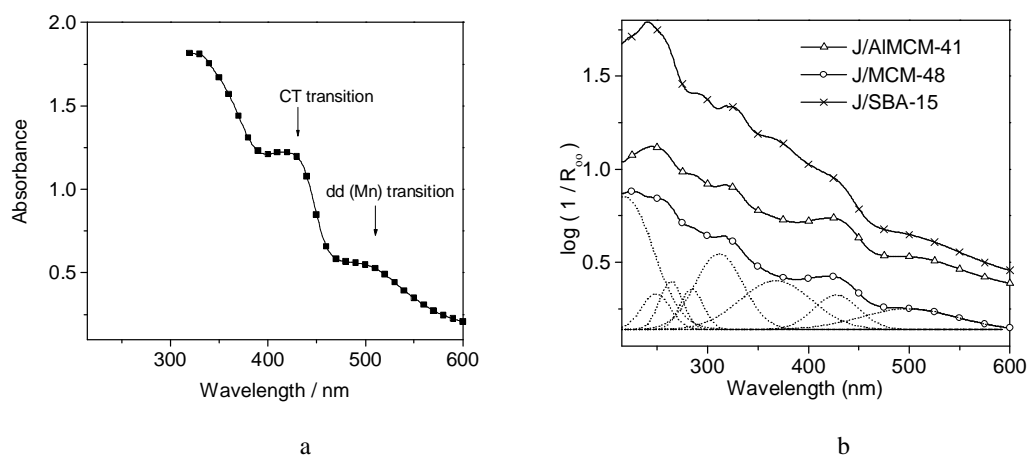


Fig. 7. UV-vis spectra of A) Jacobsen complex in DCM solution (0.580 mol/L); B) composite samples. Dotted lines represent a possible decomposition of the corresponding spectrum (sample J/MCM-48).

In fact, the importance of the complex bonding to the surface, whether the complex is attached to the surface through the chiral equatorial tetradentate salen ligand or via the apical ligand, has been recently revealed [24].

Table 2. Position (nm) of characteristic bands in composites containing Jacobsen complex in comparison with related complexes.

Absorbing species	CT	dd	Ref.
[(R,R)-N,N'-bis(3- <i>tert</i> -butyl-5-vinylsalicylidene)-1,2-cyclohexanediamine] manganese(III) chloride	412	500	[24]
[(R,R)-N,N'-bis(3,5-di- <i>tert</i> -butylsalicylidene)-1,2-cyclohexanediamine] manganese(III)6-heptene-carboxylate	412	510	[24]
[(R,R)-N,N'-bis(3,5-di- <i>tert</i> -butylsalicylidene)-1,2-cyclohexanediamine] manganese(III)10-undecenoxide	420	500	[24]
J/SiMCM-48	435	503	This work
J/SiSBA-15	427	486	This work
J/AlSBA-15	426	486	This work
J/AIMCM-41(2)	429	479	This work

4. Conclusions

Jacobsen complex is loaded in nanoporous molecular sieves as SBA-15 and MCM-48 by impregnation. Maximum loading (after leaching) for nanoporous materials with pores larger than 2 nm was 1.5 % in weight.

Strong guest-host interaction between Jacobsen complex and the walls of the molecular sieves leads to strong bonding as shown by in situ IR, UV-vis and TA measurements.

Thermogravimetric measurements allowed estimating the amount of the complex in the composites.

Siliceous nanoporous materials have a weaker interaction than Al containing forms.

IR spectra in KBr are irrelevant for the samples with low loading degree.

Diffuse reflectance UV-vis spectra showed the typical spectra associated with the species of the Mn(III) salen complex.

Acknowledgements

The authors are indebted to Romanian Ministry of Education and Research (MEdC) for the financial support (Project 59/C2) under CERES Programme.

References

- [1] R. A. Johnson, K. B. Sharpless, in "Catalytic Asymmetric Synthesis" (I. Ojima, Ed.), Ch. 4.1, p. 103. VCH, New York, 1993.
- [2] E. N. Jacobsen, A. Pfaltz, N. Yamamoto, in "Comprehensive Asymmetric Catalysis," Vol. II, p. 649. Springer-Verlag, Berlin, 1999.
- [3] (a) W. Zhang, J. L. Loebach, S. R. Wilson, E. N. Jacobsen, *J. Am. Chem. Soc.* **112**, 2801 (1990); (b) E. N. Jacobsen, W. Zhang, A. R. Muci, J. R. Ecker, L. Deng, *J. Am. Chem. Soc.* **113**, 7063 (1991).
- [4] (a) T. Irie, K. Noda, N. Matsumoto, T. Katsuki, *Tetrahedron Lett.* **31**, 7345 (1990); (b) T. Katsuki, *Coord. Chem. Rev.* **140**, 189 (1995).
- [5] S. B. Ogunwumi, T. Bein, *Chem. Commun.* 901 (1997).
- [6] M. J. Sabater, A. Corma, A. Doménech, V. Fornés, H. García, *Chem. Commun.* 1285 (1997).
- [7] (a) J. M. Fraile, J. I. García, J. Massam, J. A. Mayoral, *J. Mol. Catal. A* **136**, 47 (1998).
- [8] F. Minutolo, D. Pini, A. Petri, P. Salvadori, *Tetrahedron: Asymmetry* **7**, 2293 (1996).
- [9] L. Frunza, H. Kosslick, H. Landmesser, E. Höft, R. Fricke, *J. Mol. Catal.* **123**, 179 (1997)
- [10] K. B. M. Janssen, I. Laquiere, W. Dehaen, R. F. Parton, I. F. J. Vankelecom, P. A. Jacobs, *Tetrahedron: Asymmetry* **8**, 3481 (1997).
- [11] L. Canali, D.C. Sherrington, *Chem. Soc. Rev.* **28**, 85 (1999).
- [12] C. E. Song, E. J. Roh, B. M. Yu, D. Y. Chi, S. C. Kim, K. J. Lee, *Chem. Commun.* 615 (2000).
- [13] T. S. Reger, K. D. Janda, *J. Am. Chem. Soc.* **122**, 6929 (2000).
- [14] F. Bigi, L. Moroni, R. Magi, G. Sartori, *Chem. Commun.* 716 (2002).
- [15] J. S. Beck, J. C. Vartuli, W. J. Roth, M. E. Leonowicz, C. T. Kresge, K. D. Schmitt, C. T. W. Chu, D. H. Olson, E. W. Sheppard, S. B. McCullen, J. B. Higgins, J. L. Schlenker, *J. Am. Chem. Soc.* **114**, 10834 (1992).
- [16] C. T. Kresge, M. E. Leonowicz, W. J. Roth, J. C. Vartuli, J. S. Beck, *Nature* **359**, 710 (1992).
- [17] D. Zhao, Q. Huo, J. Feng, B. F. Chmelka, G. D. Stucky, *J. Am. Chem. Soc.* **120**, 6024 (1998).
- [18] P. Yang, D. Zhao, D. Margolese, G. D. Stucky, *Nature* **396**, 152 (1998).
- [19] S. S. Kim, T. R. Pauly, T. J. Pinnavaia, *Chem. Commun.* 1661 (2000).
- [20] A. Monnier, F. Schuth, Q. Huo, D. Kumar, D. Margolese, R. S. Maxwell, G. D. Stucky, M. Krishnamurty, P. Petroff, A. Firouzi, M. Janicke, B. F. Chmelka, *Science* **261**, 1299 (1993).
- [21] J. F. Larrow, E. N. Jacobsen, *J. Org. Chem.* **59**, 1939 (1994).
- [22] D. J. Gravert, J. H. Griffin, *J. Org. Chem.* **58**, 820 (1993).
- [23] M. M. Bhadbhade, D. Srinivas, *Inorg. Chem.* **32**, 6122 (1993).
- [24] I. Domínguez, V. Fornés, M. J. Sabater, *J. Catal.* **228**, 92 (2004).
- [25] A. B. P. Lever, *Inorganic Electronic Spectroscopy*, Elsevier, Amsterdam, 1968.